



Nitrate Removal from Aqueous Solution by Hexadecyltrimethylammonium Bromide-Modified Clinoptilolite

S. DIKMEN* and E. YORUKOGULLARI

Department of Physics, Anadolu University, Eskisehir, Turkey

*Corresponding author: Fax:+ 90 222 3204910; Tel: +90 222 3350585; E-mail: sdikmen@anadolu.edu.tr

(Received: 17 August 2010;

Accepted: 18 February 2011)

AJC-9632

In the first stage of study, detailed characterization studies were performed on clinoptilolite-rich tuff mined from the Gördes/Manisa region (Turkey). The physical and chemical properties were determined using instrumental analysis techniques, including XRD, XRF, SEM, DTG-DTA and specific surface area. In the second stage, modification of clinoptilolite-rich tuff surface with hexadecyltrimethylammonium bromide (HDTMA) to improve the adsorption efficiency of nitrate was performed using a batch equilibration method. The surface modification of clinoptilolite with a surfactant was examined using the FT-IR spectroscopic technique and equilibrium data. The Langmuir and Freundlich adsorption models were applied to describe the equilibrium isotherms and the isotherm constants were also determined. The equilibrium data are fitted to the Freundlich adsorption isotherm. The kinetic models were used to describe the kinetic data and the rate constants were evaluated. The experimental data fitted well the pseudo-second-order kinetic model and also followed the intraparticle diffusion model up to 1 h.

Key Words: Adsorption, Clinoptilolite, Nitrate, Surfactant.

INTRODUCTION

The effects of water pollution are far-reaching and affect not only the environment, but human beings and animals besides. The major reasons of the water pollution are the arising agricultural and industrial activities. Nitrate is a wide spread contamination of ground and surface waters worldwide. The accumulation of nitrate in the environment results mainly from: discharges of untreated municipal and industrial wastewater runoff septic tanks, processed food and dairy and meat products decomposition of decaying organic matter buried into ground^{1,2}. In addition, the extensive use of nitrogen-containing fertilizers is the most significant anthropogenic sources of nitrate contamination in groundwater³. Nitrogen compounds are highly soluble in water and hence easily mobile in the environment. When quantity of nitrogen added to the soil exceed the amount that the plants can use, the excess nitrate does not get much adsorbed by soil particles and ultimately accumulates into the groundwater^{2,3}. Although nitrates are relatively harmless, their conversion to nitrites or other N-nitroso compounds in the body may produce toxic products. Increased fertilizer use in agriculture may have amplified the yield, but also showed deleterious effect in the soils such as increased salinity and alkalinity⁴. A high level of nitrate ions in drinking water can cause lots of health problems. Several studies reveal that excess nitrate in drinking water can cause

methemoglobinemia also called a "blue baby syndrome" all infants under six month^{5,6}. Yang *et al.*⁷, has stated that the diseases such as stomach, colon cancer and lymphoma based on high level of the nitrate in drinking water. The continuous consumption of water containing high nitrate may cause several health hazardous² such as vascular dementia, secretive functional disorders of the intestinal mucosa, Non-Hodgkin's lymphoma, hypertrophy of thyroid, *etc.* Besides, nitrate becomes nitrite through biodegradation and the nitrite occurred creates the compound of N-nitroso which carries the risk of cancer through reacting with the secondary and tertiary amine and amides which are present in the water and foods⁸.

In order to ensure public health from the adverse effects of high nitrate level, World Health Organization (WHO) established a maximum contaminant level of 50 mg L⁻¹. According to US Environmental Protection Agency (EPA) drinking water must contains not more than 45 mg L⁻¹-NO₃^{-9,10}.

There are various conventional processes such as filtration, chlorination, coagulation, *etc.*, for water treatment, but they are not enough for the removal of nitrate. Therefore, a number of treatment technologies have been used such as biological denitrification, ion exchange, reverse osmosis, chemical reductants, distillation and electro dialysis¹¹. Mechanical filters of various types and standard water softeners do not remove nitrate-nitrogen¹². Biological denitrification is one of the most

efficient methods for removal of excessive amounts of nitrates from ground water. Unfortunately, biological denitrification can produce excessive biomass and soluble microbial products which require subsequent treatment, especially when heterotrophic bacteria are used¹³.

The adsorbents used for nitrate adsorption are the active carbon and the resins⁵. However, as the cost of these adsorbents are so high, the researchers have gone towards the studies that deal with the modification of clay and zeolite minerals which are abundant and also low cost for the removal of the organic and anionic pollutants¹⁴. Most of the zeolite minerals are characterized by high specific surface areas and high cation exchange capacities (CECs). Their rigid three-dimensional structures make them free of the shrink/swell behaviour associated with smectite clays. For these reasons, zeolite can offer superior adsorption properties and have found use as molecular sieves and sorbents in wastewater treatment^{15,16}. As natural zeolites carry a net negative charge in the crystal lattice, they show little interest for anionic type pollutants without previous modification^{17,18}. Surfactant-modified zeolite (SMZ) and clay (SMC) minerals are frequently studied by many researchers because of the unique adsorptive properties of the modified material. Using these modified materials was focused on removal of hydrophobic organic contaminants from water¹⁹⁻³¹. Ozcan *et al.*³¹, indicated that both natural and surfactant-modified sepiolite is effective sorbents for the removal of anionic contaminants. However, the surfactant-modified sepiolite (453 mmol kg⁻¹) was more effective than the unmodified sepiolite (408 mmol kg⁻¹) in this respect. Another study was evaluate to the effect of different surfactants (*i.e.*, HDTMA and CPB) on the adsorbing characteristics of surface modified natural zeolite for the separation of petroleum monoaromatic compounds (*i.e.*, benzene, toluene, ethyl benzene and xylene (BTEX)) from contaminated water. CPB-modified zeolite showed a higher adsorption capacity for all of the monochromatic compounds than HDTMA-modified zeolite³².

Clinoptilolite is one of the natural zeolite minerals which are still the most abundant reserves both in the world and in Turkey. The presence of 4.5 million tons of natural zeolite of high quality, mainly those of clinoptilolite in Turkey, created an impetus for the utilization of clinoptilolite in wastewater treatment³³. To our best of knowledge, systematic studies on the modification of clinoptilolite originated from Turkey (Manisa, Gördes) for nitrate anions removal purpose has not yet existed. The adsorption capacity of modified clinoptilolite for the removal of nitrate was examined in this work as well as the effect of initial concentration, pH and contact time were investigated.

EXPERIMENTAL

The adsorbent material used in the study taken from a sedimentary deposit in Gördes region Western Anatolia, Turkey. Sample was ground and sieved to -90 µm. This selected fraction was washed with deionized water to remove very fine particles that may cause operational problems. The clinoptilolite sample was washed, then dried at 120 °C overnight in an oven prior to use. Its mineralogical (Bruker D8-Advance, X-ray diffraction), chemical (Bruker Tiger S8, X-ray fluore-

scence), density (Quantachrome, ultrapycnometer 1000), specific surface area and pore volume (Quantachrome Nova-2200) analyses were carried out and the results were given in Table-1 and Fig. 1. The clinoptilolite surface was also examined using a scanning electron microscope (Cam Scan S4) after Au-Pd coating (Fig. 2). The FT-IR spectra were recorded (KBr) on a Perkin Elmer spectrum 100 FT-IR spectrometer to observe surface modification (Fig. 4). In addition to, the unmodified clinoptilolite, HDTMA-modified clinoptilolite and pure surfactant were characterized by thermal analysis (DTG/DTA). Thermal analysis was performed on a Setaram, Setsys Evolution. Unmodified clinoptilolite, HDTMA-clinoptilolite and pure surfactant were heated in the range at 30-900 and 25-400 °C, respectively at a heating rate of 10 °C min⁻¹ (Fig. 5a-c).

TABLE-1
CHEMICAL, MINERALOGICAL COMPOSITION AND SOME
PHYSICAL PROPERTIES OF CLINOPTILOLITE SAMPLE (wt %)

Chemical analysis	
Component	Value
SiO ₂	70.90
Al ₂ O ₃	12.4
CaO	2.18
MgO	0.83
Fe ₂ O ₃	1.41
K ₂ O	2.46
Na ₂ O	0.38
TiO ₂	0.07
MnO	< 0.01
BaO	0.02
LOI*	9.34
Total	100.00
Mineralogical analysis	
Clinoptilolite	90.5
Feldspar	3.8
Quartz	4.3
Muscovite	1.4
Physical properties	
Density (g/cc)	2.160
Surface area (BET method) (m ² /g)	48.060
Average pore width (DR method) (nm)	9.660
Pore volume (cc/g)	0.044

*LOI: Loss on ignition.

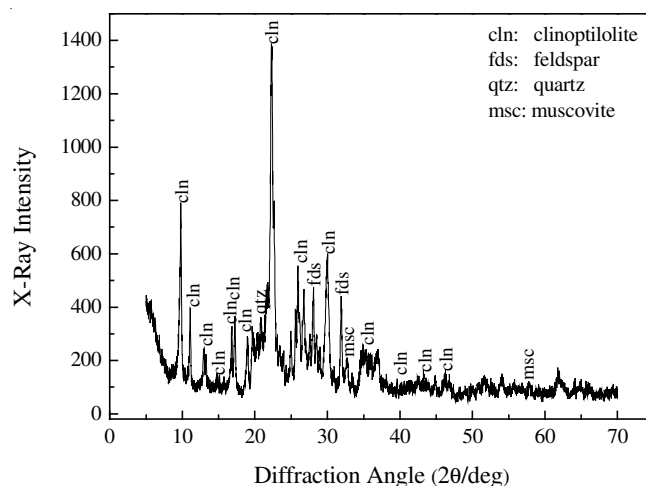


Fig. 1. X-Ray diffraction pattern of the clinoptilolite

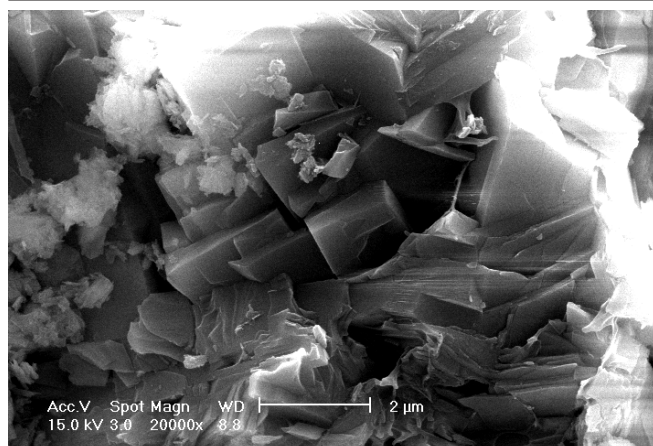


Fig. 2. SEM image of the clinoptilolite

Preparation of the HDTMA-clinoptilolite: Hexadecyltrimethylammonium bromide (HDTMA-Br, $C_{16}H_{33}(CH_3)_3NBr$, Sigma-Aldrich Cor., 99 % purity) was used in this study. The quaternary amine HDTMA cationic surfactant consists of permanently charged trimethylammonium head group attached to a 16-carbon chain tail group. Its molecular weight is 364.46 g/mol and melting point is $-235\text{ }^\circ\text{C}$. The bromide salt of surfactant was selected because Li and Bowman³⁴ reported that the adsorption of HDTMA-Br onto clinoptilolite is more stable than that of HDTMA- H_2SO_4 and HDTMA-Cl. The procedure for preparing the modified clinoptilolite is shown³⁵ in Fig. 3.

Adsorption experiments: To determine the adsorption equilibrium and maximum adsorption capacity nitrate concentration of 50-250 mg L^{-1} were prepared using NaNO_3 . The stock solutions of 250 mg L^{-1} of nitrate were prepared with deionized water of less than 3 $\mu\text{mhos cm}^{-1}$ conductivity. Nitrate solutions of 50 mL at different concentrations in the range of 50-250 mg L^{-1} were removed from their stock solutions and transferred into 50 mL tubes containing 1 g of HDTMA-clinoptilolite. They were conditioned in an incubator in order to reach equilibrium, followed by centrifugation at 3500 rpm. The supernatants were analyzed by UV-spectrophotometer (Hach-Lange, DR5000) using NitroVer 5 test kits. The amount of nitrate in the solid phase, q (mg g^{-1}), was calculated using the equation:

$$q = \frac{(C_i - C_e)}{m} V \quad (1)$$

where C_i and C_e = initial and equilibrium concentrations of nitrate (mg L^{-1}), respectively. V = solution volume (L) and m = weight of adsorbent (g).

RESULTS AND DISCUSSION

Mineralogical and physico-chemical properties: The mineralogical compositions of the natural clinoptilolite were determined using powder XRD method (Fig. 1). The composition of natural clinoptilolite was determined on the basis of the basal reflections at 8.96 (9.88°), 7.91 (11.19°), 6.78 (13.06°), 5.93 (14.94°), 5.33 (16.63°), 5.11 (17.36°), 3.97 (22.36°), 3.55 (25.05°) and 2.93 \AA (30.40°). It was found that the largest intensity peaks correspond to clinoptilolite as the dominating species. Quartz, feldspar and muscovite were also

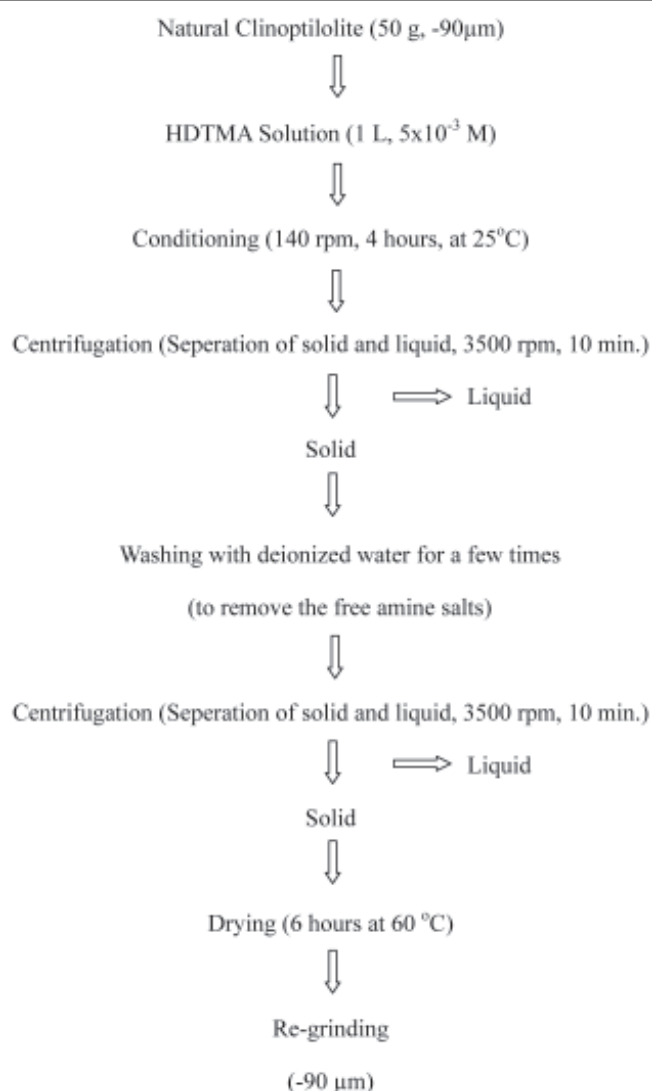


Fig. 3. Flowsheet for preparing modified clinoptilolite³⁵

identified as an impurity. According to the mineralogical and chemical analysis results, the zeolite sample can be accepted as clinoptilolite tuff (Table-1). Also, the Si/Al ratio of the sample as calculated from this composition is 5.71, which is within the typical range of 4.0-5.5 given for clinoptilolite³⁶. Physical properties of the clinoptilolite are within the range of values reported for clinoptilolite in previous works³⁷⁻³⁹. Its relatively high specific surface area value attracts attention which is one of the important properties for adsorption process. The surface image of the Gördes clinoptilolite sample, obtained by SEM, is shown in Fig. 2. The clinoptilolite crystals occur partially developed crystalline as euhedral to sub-hedral plates and conglomerates of compact crystals different from other of the zeolite crystals that correspond to certain impurities such as feldspar and quartz.

FT-IR analysis: The spectra of the unmodified clinoptilolite and surfactant-modified clinoptilolite are given in Fig. 4. In the FT-IR spectrum of unmodified clinoptilolite four groups of bands are present. The bands due to the presence of zeolitic water ($3700\text{-}1600\text{ cm}^{-1}$). The bands related to internal Si-O-Si and Si-O-Al vibrations in tetrahedral or alumina- and silica-oxygen bridges ($1200\text{-}400\text{ cm}^{-1}$). The bands due to pseudo-lattice vibrations of structural units ($700\text{-}500$

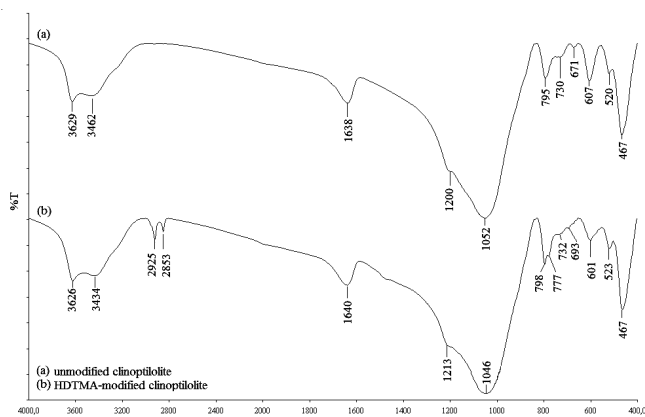


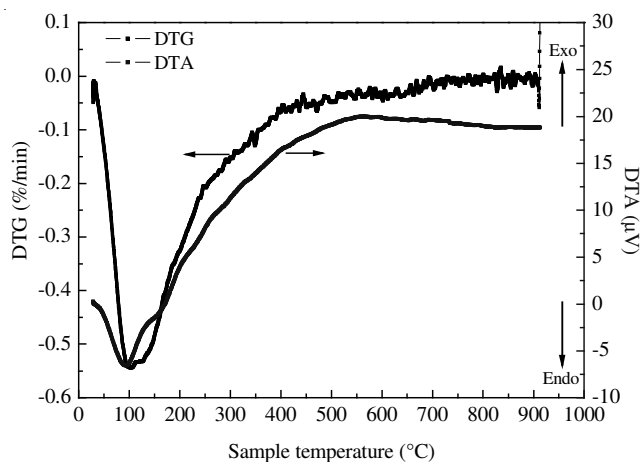
Fig. 4. FTIR spectra of (a) unmodified clinoptilolite (b) HDTMA-modified clinoptilolite

cm^{-1}). The bands due to T-O double ring bending ($500\text{--}400\text{ cm}^{-1}$)⁴⁰⁻⁴².

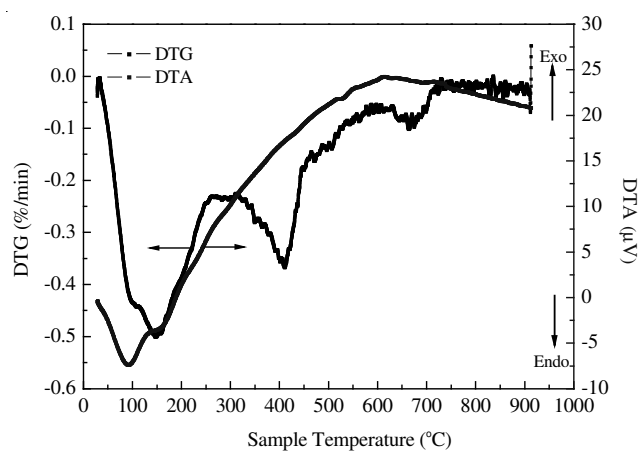
FT-IR spectrum of the unmodified clinoptilolite display bands in the region $3700\text{--}3400\text{ cm}^{-1}$, with a shoulder at 3629 cm^{-1} , the band at 1638 cm^{-1} (H-O-H bending) and the broad band in the range of $1300\text{--}990\text{ cm}^{-1}$ with a shoulder at 1200 cm^{-1} due to stretching vibrations Si-Al-O.

Two bands were observed at 795 and 730 cm^{-1} due to and Al-O-Si and Si-O-Si vibrations, respectively. There was a peak at 671 cm^{-1} due to 4 or 6-membered ring vibrations of SiO_4 or AlO_4 tetrahedra for the ordered crystal structure and a band at 607 cm^{-1} due to stretching of the intertetrahedral bonds for the ordered crystal structure (Fig. 4a)⁴³. The FT-IR spectrum for the C-H stretching band region of in 5 mM HDTMA solution is shown in Fig. 4b. A pair of characteristic bands at 2925 and 2853 cm^{-1} present in surfactant-modified clinoptilolite can be assigned to the symmetric and asymmetric stretching vibrations of the methylene group [$\gamma_s(\text{CH}_2)$, $\gamma_{as}(\text{CH}_2)$]⁴⁴. In addition to, shifts in wave numbers of these bands are observed and they probably could display partial displacement of water molecules by adsorbed HDTMA-clinoptilolite^{45,46}.

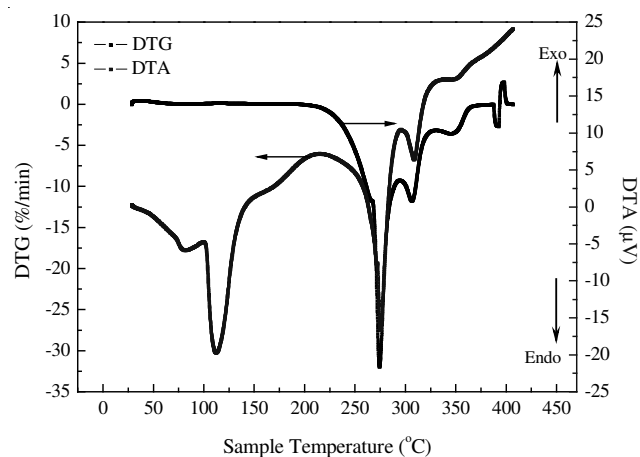
Thermal analysis: Thermal analysis is the common method used to study the adsorption of organic compounds by natural clays and zeolites⁴⁷. Natural zeolite modified with different concentrations of HDTMA (below and above monolayer coverage) by high resolution thermogravimetric analysis (HR-TGA) and demonstrated that HR-TGA pyrolysis temperatures should be higher for samples with more strongly bound HDTMA, such as that bound with both coulombic and van der Waals forces at-sub-monolayer coverages. If HDTMA is bound only by hydrophobic forces, such as in a bilayer, the pyrolysis temperature should be considerably lower⁴⁸. The DTA and DTG curves of natural clinoptilolite, HDTMA-modified clinoptilolite and pure HDTMA are given in Fig. 5a-c. The DTG curve of natural form exhibited a peak at temperature of $100\text{ }^\circ\text{C}$ that was due to physically adsorbed water. The water found within the framework is known as zeolitic water. This curve can be observed that the mass loss decreased continuously until it leveled off at $550\text{ }^\circ\text{C}$. The total mass variation for unmodified clinoptilolite was 10.07% of the initial mass. The DTG curve of the HDTMA-modified presented four peaks at temperatures of 100 , 148 , 405 and $670\text{ }^\circ\text{C}$. The first and second peaks were due to desorption of free



(a)



(b)



(c)

Fig. 5. Differential thermogravimetric (DTG) and differential thermal analysis (DTA) of (a) unmodified clinoptilolite, (b) HDTMA-modified clinoptilolite and (c) pure HDTMA

water. The total mass variation due to surfactant decomposition was 14.56% . The peaks at 405 and $670\text{ }^\circ\text{C}$ were due to oxidation of the surfactant, as well as to water coordinated to the cations remaining within clinoptilolite channels. The intensity of the peaks in the temperature region $50\text{--}200\text{ }^\circ\text{C}$ was lower than for natural clinoptilolite due to the hydrophobicity surface as it can be seen from Fig. 5-a and b. The DTA curve of the natural clinoptilolite (Fig. 5a) exhibited on endothermic

peak at 95 °C with a shoulder at 155 °C. This dehydration peak was changed after ion exchange of cations at the clinoptilolite surface with cationic surfactant, confirming that desorption of physically adsorbed water from partially covered surface is a major thermal reaction in this region. The DTG curve of pure HDTMA (Fig. 5c) represented mass variation in the range of 200-350 °C, which corresponds to the loss of the 98 % of organic compound. This mass variation is related to exothermic peaks at temperatures of 275 and 330 °C, also three endothermic DTA peaks are noticed^{39,47}. The two endothermic peaks occurring at 80 and 112 °C may be results of some structural rearrangements in alkyl chains of surfactant. This is the process of "kink" formation known as chain melting, which is based on the introduction on conformational isomerization *via* rotation about the C-C bonds. These bring one or more *gauche* bonds to *trans* bonds in the alkyl chains. The DTA peak at 275 °C occurs with DTG peak due to the melting and pyrolysis of the pure HDTMA⁴⁹.

Effect of contact time: The effect of contact time on the amount of nitrate adsorbed onto HDTMA-clinoptilolite was examined at 50 mg L⁻¹ initial concentration of nitrate. As can be seen from Fig. 6, initially the rate of adsorption was rapid and then slowed down until 3 h. The maximum adsorption capacity of nitrate onto adsorbent was reached at 1 h. Thus, it was obtained as the optimum contact time.

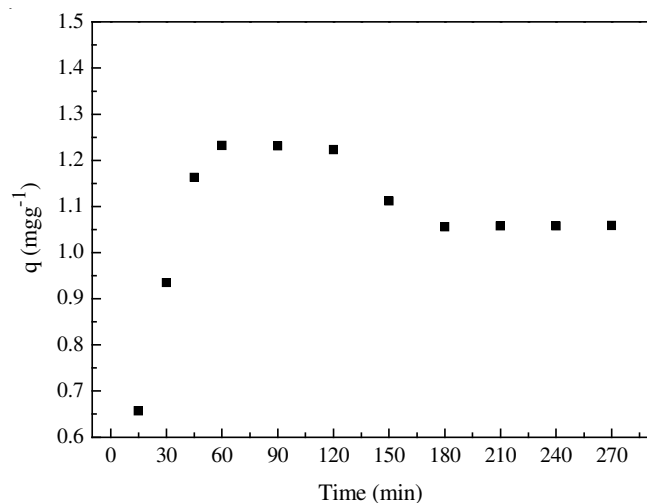


Fig. 6. Effect of contact time for the nitrate adsorption onto HDTMA-clinoptilolite (C_0 : 50 mg L⁻¹, T: 25 °C, agitation speed: 140 rpm, adsorbent dosage: 20 g L⁻¹)

Effect of pH on the adsorption capacity: Adsorption of nitrate onto HDTMA-clinoptilolite was carried out for the examination of the effect of pH in 2-8 range and it was found that the adsorption decreased with an increase in pH (Fig. 7). This clearly shows that the adsorption capacity depend upon the pH of the solution, which affects the surface charge of the adsorbent and the degree of ionization and speciation of adsorbate. The higher adsorption capacities of the nitrate ions onto adsorbent were observed at lower pH values due to electrostatic interaction between the negatively charged nitrate ions and positively charged adsorption sites. On the contrary, when the pH of solution increases, the number of negatively charged sites increases while the number of

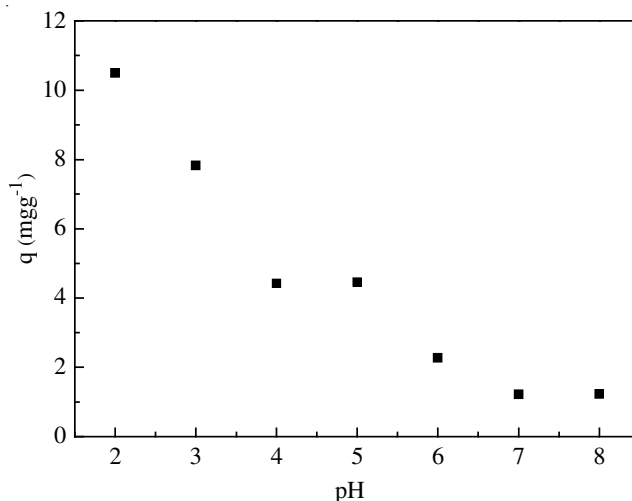


Fig. 7. pH effect for nitrate adsorption onto HDTMA-clinoptilolite. (C_0 : 50 mg L⁻¹, T: 25 °C, agitation speed: 140 rpm, adsorbent dosage: 20 g L⁻¹)

positively charged sites decreases. The abundance of negatively charged surface sites does not prefer nitrate anions due to electrostatic repulsion. There are also no exchangeable anions on the outer surface of the HDTMA-clinoptilolite at higher pH values and consequently the adsorption decreases.

Adsorption isotherms: The plot of q_e versus C_e for the adsorption of nitrate onto HDTMA-clinoptilolite was drawn (Fig. 8) and applied to Langmuir (the isotherm was removed) and Freundlich isotherm (Fig. 9). The equilibrium adsorption isotherm is one of the most important data to understand the mechanism of the adsorption systems. Several isotherm equations are available and two important isotherms are selected in this study, which are namely the Freundlich⁵⁰ and Langmuir⁵¹ isotherms.

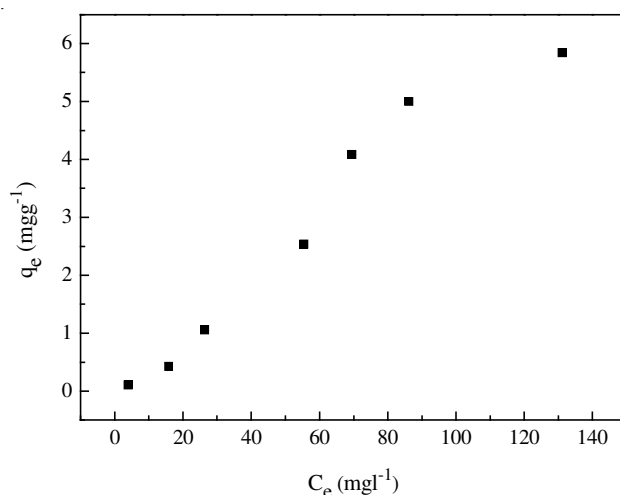


Fig. 8. Nitrate adsorption of the HDTMA-clinoptilolite (T: 25 °C; agitation speed: 140 rpm, adsorbent dosage: 20 g L⁻¹)

The Freundlich isotherm is an empirical equation employed to describe heterogeneous systems. A linear form of the Freundlich equation is

$$\log q_e = \log K_F + \frac{1}{n} (\log C_e) \quad (2)$$

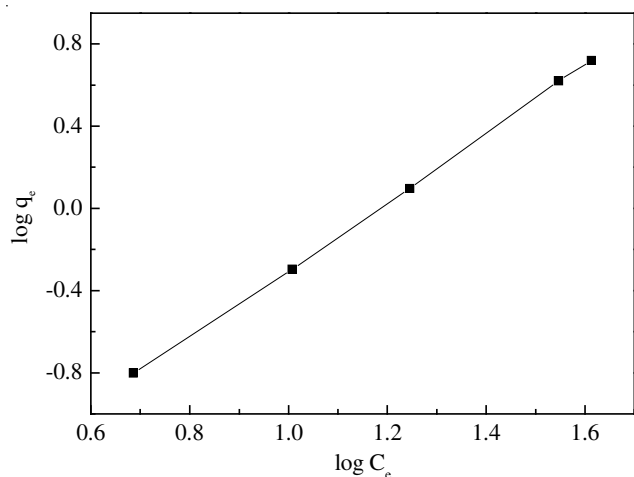


Fig. 9. Freundlich plot for the adsorption of nitrate onto HDTMA-clinoptilolite

where K_F ($L g^{-1}$) and n are Freundlich adsorption isotherms constants, being indicative of the extent of the adsorption and the degree of non-linearity between solution concentration and adsorption, respectively. The plot of $\log q_e$ versus $\log C_e$ for the adsorption of nitrate onto HDTMA-clinoptilolite (Fig. 9) was employed to generate the intercept value of K_F and the slope of $1/n$.

Langmuir adsorption isotherm assumes that adsorption takes place at specific homogeneous sites within the adsorbent and has found successful application in many adsorption processes of monolayer adsorption. The linear form of the Langmuir isotherm equation is represented by the following equation:

$$\frac{1}{q_e} = \frac{1}{q_{\max}} + \left(\frac{1}{q_{\max} K_L} \right) \frac{1}{C_e} \quad (3)$$

where q_e = equilibrium concentration of the adsorbent $mg g^{-1}$, C_e = equilibrium concentration in the solution ($mg L^{-1}$), q_{\max} = monolayer adsorption capacity of the adsorbent ($mg g^{-1}$) and K_L = Langmuir adsorption constant ($L mg^{-1}$) and related to the free energy of adsorption. The plots of $(1/q_e)$ versus $(1/C_e)$ for the adsorption of nitrate onto HDTMA-clinoptilolite has not given straight line of slope $1/q_{\max} K_L$ and intercept $1/q_{\max}$.

The values of the Langmuir constant (K_L) and the monolayer capacity of adsorbent (q_{\max}), Freundlich constant (K_F) and (n), the correlation coefficients for Langmuir (r_L^2) and for Freundlich (r_F^2) are listed in Table-2.

TABLE-2 ADSORPTION ISOTHERM CONSTANTS FOR THE ADSORPTION OF NITRATE ONTO HDTMA-CLINOPTILOLITE					
Langmuir isotherm			Freundlich isotherm		
q_{\max} ($mg g^{-1}$)	K_L ($L g^{-1}$)	r_L^2	n	K_F ($L g^{-1}$)	r_F^2
12.140	7.98×10^{-3}	0.757	0.720	0.02	0.985

TABLE-3 KINETIC PARAMETERS FOR THE ADSORPTION OF NITRATE ON HDTMA-CLINOPTILOLITE						
Pseudo-first-order			Pseudo-second-order			Intraparticle diffusion
q_1 ($mg g^{-1}$)	k_1 (min^{-1})	r_1^2	q_2 ($mg g^{-1}$)	k_2 (min^{-1})	r_2^2	k_p ($mg g^{-1} min^{1/2}$)
1.234	11.213	0.731	1.234	0.046	0.983	0.0768
						r_p^2
						0.727

Adsorption kinetics: Three kinetic models (the first-order equation, the pseudo-second-order equation and intraparticle diffusion equation) were applied to fit the experimental data to examine the adsorption kinetic model equation.

The pseudo-first-order kinetic model equation^{52,53} is given as:

$$\frac{t}{q_t} = \left(\frac{k_1}{q_{\max}} \right) \left(\frac{1}{t} \right) + \frac{1}{q_{\max}} \quad (4)$$

where q_{\max} = maximum adsorption capacity ($mg g^{-1}$), q_t = amount of nitrate adsorbed at times t , k_1 (min^{-1}) is the pseudo-first-order rate constant (min^{-1}) for the adsorption process.

The pseudo-second-order kinetic model^{54,55} is expressed as:

$$\frac{t}{q_t} = \left(\frac{1}{k_2 q_2^2} \right) + \frac{1}{q_2} t \quad (5)$$

The intraparticle diffusion equation⁵⁶ can be written as follows:

$$q_t = k_p t^{1/2} + C \quad (6)$$

where q_2 and q_1 = amounts of the nitrate adsorbed at equilibrium and at time t ($mg g^{-1}$), k_2 = equilibrium rate constant of the pseudo-second-order model for the adsorption process ($g mg^{-1} min^{-1}$), C = intercept and k_p = intraparticle diffusion rate constant ($mg g^{-1} min^{1/2}$). The plot of t/q_t versus t for the pseudo-second-order for the adsorption of nitrate onto HDTMA-clinoptilolite has also been examined to obtain the rate parameters (Fig. 10). All the kinetic data of nitrate were calculated from these equations and listed in Table-3. From this table, the correlation coefficients (r_1^2) for the pseudo-first-order kinetic model was 0.731. The correlation coefficients (r_2^2) for the pseudo-second-order kinetic model was 0.983 for adsorbent. This statement shows that this adsorption system does not fit pseudo-first-order reaction. It fits the pseudo-second-order kinetic model. According to the intra-particle diffusion model, q_t versus the square root of time, $t^{1/2}$, (Fig. 11) should be linear if intraparticle diffusion is involved in the adsorption process and this line passes through the origin the intraparticle diffusion is the rate controlling step⁵⁷. From Fig. 11, the experimental data has not been across the zero point, which indicated that the diffusion is main rate-controlling step. When the plot is not through the origin, this is indicative of some degree of boundary layer control and this further show that intraparticle diffusion is not only rate limiting step, but also other kinetic models may control the rate of adsorption, all which may be operating simultaneously⁴⁴. The initial portion of the plot seems to be due to boundary layer adsorption and the linear portion to intraparticle diffusion, with the plateau corresponding to equilibrium. The plot has not passed through

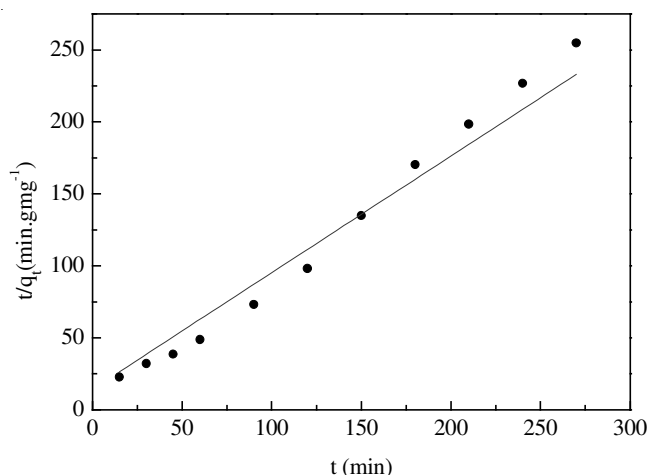


Fig. 10. Pseudo-second-order kinetic plot for the adsorption of nitrate onto HDTMA-clinoptilolite

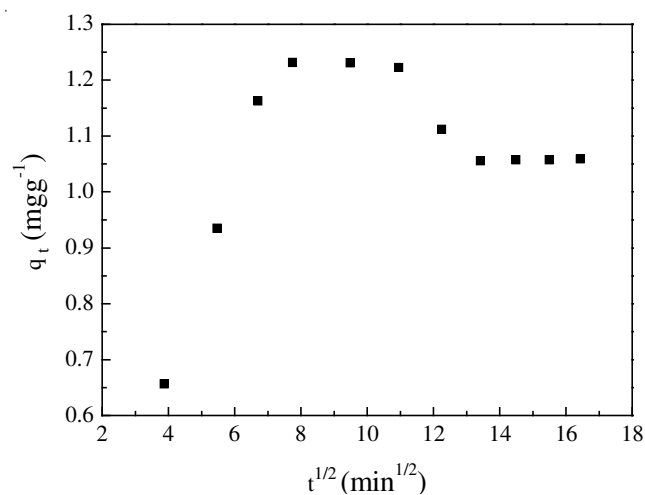


Fig. 11. Intraparticle diffusion plot for the adsorption of nitrate onto HDTMA-clinoptilolite

the origin. This shows that although intraparticle diffusion was involved in the adsorption process, it was not the rate-controlling step.

Conclusion

In present study, the results demonstrate that the surface modification of the zeolitic tuff from the Gördes Region by long-chain quaternary amine results in an organo-clinoptilolite material possessing anionic sorption properties. Because of the availability of clinoptilolite, its low cost and simple preparation can be representing as a suitable adsorbent for the removal of nitrate contamination in surface and ground waters. The surface modification of clinoptilolite was tested by using the FT-IR technique. The adsorption was found to be dependent on pH and contact time. A maximum of 10.500 mg g⁻¹ nitrate removal could be achieved at around pH 2. The maximum removal of nitrate ions by HDTMA-clinoptilolite occurred quickly (within 1 h) and efficiently. The adsorption of nitrate onto HDTMA-clinoptilolite follows the pseudo-second-order kinetic model and also fits well the intraparticle diffusion model up to 1 h, but diffusion is not the only rate-controlling step.

ACKNOWLEDGEMENTS

The authors are grateful for kindly financial support provided by Eskişehir Anadolu University via Scientific Research Projects (No. 041029 and 081029).

REFERENCES

1. S. Samatya, N. Kabay, U. Yuksel, M. Arda and M. Yuksel, *React. Func. Polym.*, **66**, 1206 (2006).
2. S. Suthar, P. Bishnoi, S. Singh, P.K. Mutiyar, A.K. Nema and N.S. Patil, *J. Hazard. Mater.*, **171**, 189 (2009).
3. E. Ledoux, E. Gomez, J.M. Monget, C. Viavattene, P. Viennot, A. Ducharme and M. Benoit, *Sci. Total Environ.*, **375**, 33 (2007).
4. A. Dogan, A. Kazankaya, M.F. Balta and F. Celik, *Asian J. Chem.*, **20**, 1191 (2008).
5. M. Chabani, A. Amrane and A. Bensmaili, *Chem. Eng. J.*, **125**, 111 (2006).
6. C.J. Mena-Duran, M.R. Sun Kou, T. Lopez and J.A. Azamar-Barrios, *Appl. Surf. Sci.*, **253**, 5762 (2007).
7. C.Y. Yang, D.C. Wu and C.C. Chang, *Environ. Int.*, **33**, 649 (2007).
8. E. Wasik, J. Bohdziewicz and M. Blaszczyk, *Process Biochem.*, **37**, 57 (2001).
9. World Health Organization: Guidelines for Drinking Water Quality, Geneva, edn. 3 (2003).
10. US Environmental Protection Agency (EPA) Integrated Risk Information System (IRIS): Nitrate (CASRN 14797-55-8), Washington (1991).
11. Y. Wang, J. Qu, H. Liu and C. Hu, *Catal. Today*, **126**, 476 (2007).
12. W.J. Hunter, In eds.: R.F. Follett and J.L. Hatfield, In Nitrogen in the Environment: Sources, Problems and Management, Elsevier Science, Amsterdam, pp. 433-453 (2001).
13. S. Ghafari, M. Hasan and M. K. Aroua, *Bioresour. Technol.*, **99**, 3965 (2008).
14. F. Akbal, *J. Environ. Manage.*, **74**, 239 (2005).
15. D.W. Breck, *Zeolite Molecular Sieves*, John Wiley, New York (1974).
16. R.M. Barrer, *Zeolites and Clay Minerals As Sorbents and Molecular Sieves*, Academic Press, London (1978).
17. E.J. Sullivan, J.W. Carey and R.S. Bowman, *J. Colloid Interf. Sci.*, **206**, 369 (1998).
18. Z. Li, C.A. Wills and K. Kniola, *Clay Clay Miner.*, **51**, 445 (2003).
19. R.S. Bowman, *Micropor. Mesopor. Mater.*, **61**, 43 (2003).
20. B. Ersoy and M.S. Celik, *Environ. Technol.*, **25**, 341 (2004).
21. G.M. Haggerty and R.S. Bowman, *Environ. Sci. Technol.*, **28**, 452 (1994).
22. B.S. Krishna, D.S.R. Murty and B.S. Jai Prakash, *Appl. Clay Sci.*, **20**, 65 (2001).
23. J. Lemic, M.R. Tomasevic-Canovic, T. Canovic, M. Djuricic and T. Stanic, *J. Colloid Interf. Sci.*, **292**, 11 (2005).
24. Z. Li and R.S. Bowman, *J. Dispersion Sci. Technol.*, **19**, 843 (1998).
25. Z. Li and R.S. Bowman, *Environ. Sci. Technol.*, **32**, 2278 (1998).
26. Z. Li, T. Burt and R.S. Bowman, *Environ. Sci. Technol.*, **34**, 3756 (2000).
27. Z. Li and R.S. Bowman, *Water Res.*, **35**, 3771 (2001).
28. Z. Li and H. Hong, *J. Hazard Mater.*, **162**, 1487 (2009).
29. C. Diaz-Nava, M.T. Olguin, M. Solache-Riosa, M.T. Alarcon-Herrera and A. Aguilar-Elguezabalb, *J. Hazard. Mater.*, **167**, 1063 (2009).
30. A. Özcan, E.M. Öncü and A.S. Özcan, *J. Hazard. Mater.*, **129B**, 244 (2006).
31. A. Özcan, M. Sahin and A.S. Özcan, *Adsorpt. Sci. Technol.*, **23**, 323 (2005).
32. A. Torabian, H. Kazemian, L. Seifi, G.N. Bidhendi, A.A. Azimi and S.K. Ghadiri, *Clean-Soil Air Water*, **38**, 77 (2010).
33. Y.E. Benkli, M.F. Can, M. Turan and M.S. Celik, *Water Res.*, **39**, 487 (2005).
34. Z. Li and R.S. Bowman, *Environ. Sci. Technol.*, **31**, 2407 (1997).
35. B. Ersoy, Ph.D. Thesis, Istanbul Technical University, Institute of Science, Istanbul, Turkey (2000).
36. G.V. Tsitsishvili, T.G. Andronikashvili, G.M. Kirov and L.D. Filizova, *Natural Zeolites*, Ellis Harwood, Chichester (1992).
37. A.M. Kilic and O. Kilic, *Asian J. Chem.*, **18**, 1405 (2006).
38. T. Unaldi, O. Orhun and S. Kadir, *Adsorpt. Sci. Technol.*, **27**, 615 (2009).
39. R. Leyva-Ramos, A. Jacoba-Azuara, P.E. Diaz Flores and R.M. Guerrero-Coronado, *Colloid Surf. A*, **330**, 35 (2008).
40. W. Mozgawa, Z. Fojud, M. Handke and S. Jurga, *J. Mol. Struct.*, **614**, 281 (2002).

41. K. Byrappa and B.V. Suresh Kumar, *Asian J. Chem.*, **19**, 4933 (2007).
42. P. Castaldi, L. Santona, C. Cozza, V. Giuliano, C. Abbruzzese, V. Nastro and P. Melis, *J. Mol. Struct.*, **734**, 99 (2005).
43. W. Mozgawa and W. Pichor, In eds.: A.M. Brant, V.C. Li and H. Marshall, Properties of Clinoptilolite-based Autoclaved Composites, In Proceedings of International Symp, Brittle Matrix Composites 8, Woodhead Publishing Ltd., Cambridge, U.K./Zturek RSI, Warsaw, Poland, p. 477 (2006).
44. S.Y. Lee and S.J. Kim, *Appl. Clay Sci.*, **22**, 55 (2002).
45. C. del Hoyo, C. Dorado, M.S. Rodriguez-Cruz and M.J. Sanchez-Martin, *J. Therm. Anal. Calorim.*, **94**, 227 (2008).
46. M. Rozic, D.I. Sipusic, L. Sekonavic, S. Miljanic, L. Curkovic and J. Hrenovic, *J. Colloid Interf. Sci.*, **331**, 295 (2009).
47. A. Dakovic, M. Kragovic, G.E. Rottinghaus, Z. Sekulic, S. Milicevic, S.K. Milonjic and S. Zaric, *Colloid Surf. B*, **76**, 272 (2010).
48. E.J. Sullivan, D.B. Hunter and R.S. Bowman, American Chemical Society Annual Meeting, San Francisco, USA (1997).
49. M. Majdan, S. Pikus, Z. Rzaczyńska, M. Iwan, O. Maryuk, R. Kwiatkowski and H. Skrzypek, *J. Mol. Struct.*, **791**, 53 (2006).
50. H.M.F. Freundlich, *J. Phys. Chem.*, **57**, 385 (1906).
51. I. Langmuir, *J. Am. Chem. Soc.*, **40**, 1361 (1918).
52. A. Ozcan and S. Ozcan, *J. Hazard. Mater.*, **125B**, 252 (2005).
53. Y.S. Ho and G. Mckay, *Trans. IChemE.*, **76B**, 332 (1998).
54. Y.S. Ho, D.A.J. Wase and C.F. Forster, *Water SA*, **22**, 219 (1996).
55. W.J. Weber and J.C. Morriss, *J. Sanitary Eng. Div. Am. Soc. Civ. Eng.*, 89 (1963).
56. N. Kannan and M.M. Sundaram, *Dyes Pigm.*, **51**, 25 (2001).
57. J.P. Chen, S. Wu and K.H. Chong, *Carbon*, **41**, 1979 (2003).